CHAPTER

Mixed Mode Fracture

5

Prediction of crack growth generally involves two aspects, that is, when would the crack start to grow, and along what direction. Under Mode I conditions, it is well-known that the crack grows in its original direction. The fracture criterion thus can be established using either K_I in Irwin's stress intensity factor theory, or G_I in the energy release theory including the Griffith theory. Under general mixed mode conditions, experimental observations indicate that the crack will no longer grow in its original direction and K_{II} also plays a role in crack growth. Hence, appropriate fracture criteria need to be established to predict mixed mode crack extension.

As in the Mode I fracture, both energy and near-tip stress field approaches are used in mixed mode fracture studies. In the energy balance approach, a small kink from the main crack tip is analyzed to determine the energy release rate along the direction of the kink. The crack is assumed to grow along the direction that maximizes the energy release rate. This approach requires tedious mathematical analyses for a branched crack in a stress field of combined modes.

On the other hand, phenomenological models based on the stress intensity factors at the main crack tip could be established along with experimental calibration in the stress field approach. The crack growth direction is predicted directly using the existing stress intensity factor solutions, thus avoiding the complicated analyses for branched cracks. These models include the maximum tensile stress and strain energy density criteria.

5.1 A SIMPLE ELLIPTICAL MODEL

For Mode I fracture, it is known that fracture criterion can be expressed as

$$K_I = K_{Ic} \tag{5.1}$$

or equivalently

$$G_I = G_{Ic} \tag{5.2}$$

Fracture Mechanics. DOI: 10.1016/B978-0-12-385001-0.00005-5

An extension of Eq. (5.1) to I/II mixed mode fracture is

$$F_{12}(K_I, K_{II}) = 0 \tag{5.3}$$

where F_{12} is a function of K_I, K_{II}, and some material constants. A simple-minded attempt to establish the functional form of F_{12} is to use the total energy release rate,

$$G = \frac{\kappa + 1}{8\mu}\left(K_I^2 + K_{II}^2\right) \tag{5.4}$$

to gauge the critical condition for crack growth, that is, a crack extends if

$$G = G_c \tag{5.5}$$

where G_c is the critical value of G. Substituting Eq. (5.4) into Eq. (5.5) yields

$$\left(\frac{K_I}{K_c}\right)^2 + \left(\frac{K_{II}}{K_c}\right)^2 = 1 \tag{5.6}$$

where K_c is given by

$$K_c = \sqrt{\frac{8\mu G_c}{\kappa + 1}}$$

This equation represents a circle with the radius K_c in the $K_I - K_{II}$ plane. The mixed mode fracture criterion Eq. (5.6) should include Mode I and Mode II as special cases, which means $K_{Ic} = K_{IIc} = K_c$, where K_{IIc} is the crtical value of K_{II} and is in general related to K_{Ic}.

In practice, K_I and K_{II} at fracture usually do not follow the trajectory of a circle and in general $K_{Ic} \neq K_{IIc}$. The reason is that the criterion Eq. (5.6) is based on the total energy release rate formula Eq. (5.4), which holds true only when the crack grows in its original direction. Under mixed mode conditions, however, the crack does not grow in its original direction.

An extension of Eq. (5.6) to account for the disparity between K_{Ic} and K_{IIc} is to use the following functional form of K_I and K_{II}:

$$\left(\frac{K_I}{K_{Ic}}\right)^2 + \left(\frac{K_{II}}{K_{IIc}}\right)^2 = 1 \tag{5.7}$$

This equation describes an ellipse in the $K_I - K_{II}$ plane. While K_{Ic} is the fracture toughness for Mode I, K_{IIc} is determined by best matching Eq. (5.7) with the experimental data. It is noted that the crack growth direction is not discussed in the criterion Eq. (5.7).

Combined Mode I and Mode II tests are usually carried out on a tension panel with an oblique crack as shown in Figure 5.1. The in-plane sizes of the panel are much

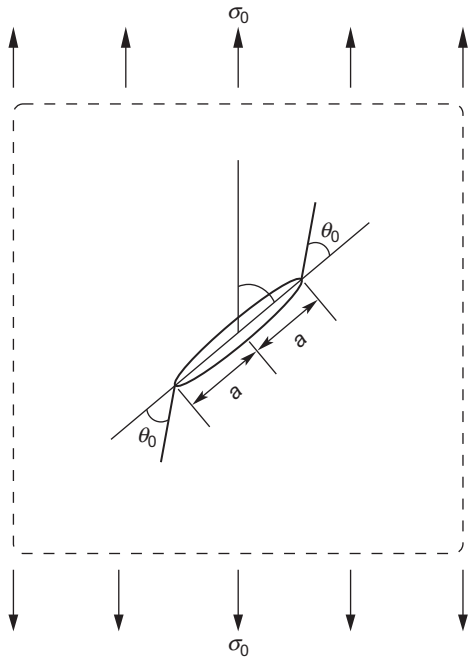

FIGURE 5.1

A tension panel with an oblique crack. The in-plane sizes of the panel are much larger than the crack length.

larger than the crack length so that the panel can be theoretically treated as an infinite one. Results of such tests on aluminum alloy sheet specimens generally confirm the applicability of Eq. (5.7) to predict mixed mode crack initiation. Figure 5.2 shows the test data for aluminum sheets (Hoskin et al. [5-1]; Pook [5-2]) and the theoretical curves from Eq. (5.7). Both plane strain and plane stress were considered.

For plane strain, the material is DTD 5050 aluminum alloy, with $K_{Ic} = 28.5$ MPa$\sqrt{\text{m}}$ and $K_{IIc} = 21.5$ MPa$\sqrt{\text{m}}$ used in Eq. (5.7). For plane stress, the material is 2024-T3 aluminum alloy and the two critical values used in the theoretical curve are 67 MPa$\sqrt{\text{m}}$ and 48.5 MPa$\sqrt{\text{m}}$, respectively. It appears from the figure that for the materials considered, K_{Ic} and K_{IIc} have an approximate correlation:

$$K_{IIc} \approx 0.75 K_{Ic}$$

Substituting this relation into Eq. (5.7) yields

$$K_I^2 + 1.78 K_{II}^2 = K_{Ic}^2$$

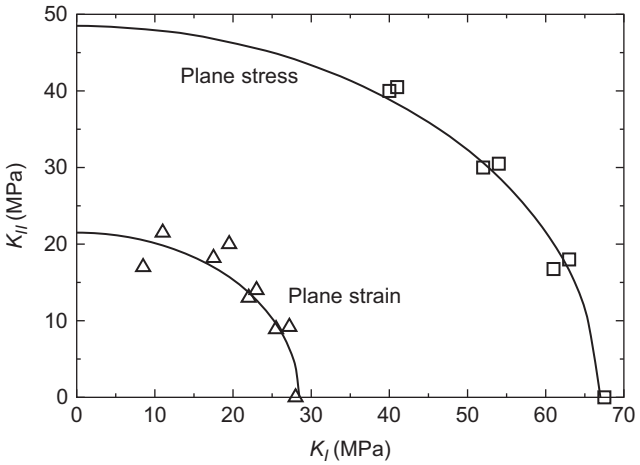

FIGURE 5.2

Experimental crack initiation data for aluminum sheets (adapted from Hoskin et al. [5-1]; Pook [5-2]) and the theoretical curves from Eq. (5.7).

5.2 MAXIMUM TENSILE STRESS CRITERION (MS-CRITERION)

Erdogan and Sih [5-3] proposed a maximum tensile stress criterion for mixed mode fracture. The criterion assumes that (1) crack extension occurs in the direction at which the circumferential stress $\sigma_{\theta\theta}$ takes the maximum with respect to θ near the crack tip, and (2) fracture takes place when $(\sigma_{\theta\theta})_{\max}$ is equal to the stress that leads to Mode I fracture.

Recall the near-tip stress field:

$$
\begin{aligned}
\sigma_{xx} &= \frac{K_I}{\sqrt{2\pi r}}\cos\frac{1}{2}\theta\left[1-\sin\frac{1}{2}\theta\sin\frac{3}{2}\theta\right] \\
&\quad -\frac{K_{II}}{\sqrt{2\pi r}}\sin\frac{1}{2}\theta\left[2+\cos\frac{\theta}{2}\cos\frac{3}{2}\theta\right] \\
\sigma_{yy} &= \frac{K_I}{\sqrt{2\pi r}}\cos\frac{1}{2}\theta\left[1+\sin\frac{1}{2}\theta\sin\frac{3}{2}\theta\right] \\
&\quad +\frac{K_{II}}{\sqrt{2\pi r}}\sin\frac{\theta}{2}\cos\frac{\theta}{2}\cos\frac{3}{2}\theta \\
\sigma_{xy} &= \frac{K_I}{\sqrt{2\pi r}}\sin\frac{\theta}{2}\cos\frac{\theta}{2}\cos\frac{3}{2}\theta \\
&\quad +\frac{K_{II}}{\sqrt{2\pi r}}\cos\frac{1}{2}\theta\left[1-\sin\frac{1}{2}\theta\sin\frac{3}{2}\theta\right]
\end{aligned}
\tag{5.8}
$$

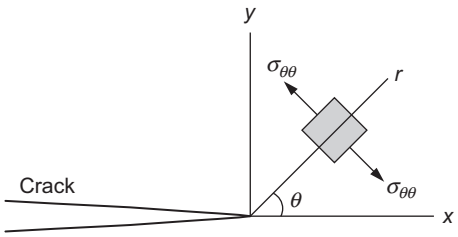

FIGURE 5.3

Coordinate systems at the crack tip and the circumferential stress $\sigma_{\theta\theta}$.

where (r,θ) are the polar coordinates centered at the crack tip as shown in Figure 5.3. Using the coordinate transformation relations of stress tensor,

$$\begin{Bmatrix} \sigma_{xx} \\ \sigma_{yy} \\ \sigma_{xy} \end{Bmatrix} = \begin{bmatrix} \cos^2\theta & \sin^2\theta & -\sin 2\theta \\ \sin^2\theta & \cos^2\theta & \sin 2\theta \\ \frac{1}{2}\sin 2\theta & -\frac{1}{2}\sin 2\theta & \cos 2\theta \end{bmatrix} \begin{Bmatrix} \sigma_{rr} \\ \sigma_{\theta\theta} \\ \sigma_{r\theta} \end{Bmatrix}$$

we obtain the near-tip stresses σ_{rr}, $\sigma_{\theta\theta}$, and $\sigma_{r\theta}$ in polar coordinates as follows:

$$\begin{aligned}
\sigma_{rr} &= \frac{K_I}{\sqrt{2\pi r}}\left(\frac{5}{4}\cos\frac{\theta}{2} - \frac{1}{4}\cos\frac{3\theta}{2}\right) \\
&\quad + \frac{K_{II}}{\sqrt{2\pi r}}\left(-\frac{5}{4}\sin\frac{\theta}{2} + \frac{3}{4}\sin\frac{3\theta}{2}\right) \\
\sigma_{\theta\theta} &= \frac{K_I}{\sqrt{2\pi r}}\left(\frac{3}{4}\cos\frac{\theta}{2} + \frac{1}{4}\cos\frac{3\theta}{2}\right) \\
&\quad + \frac{K_{II}}{\sqrt{2\pi r}}\left(-\frac{3}{4}\sin\frac{\theta}{2} - \frac{3}{4}\sin\frac{3}{2}\theta\right) \\
\sigma_{r\theta} &= \frac{K_I}{\sqrt{2\pi r}}\left(\frac{1}{4}\sin\frac{\theta}{2} + \frac{1}{4}\sin\frac{3\theta}{2}\right) \\
&\quad + \frac{K_{II}}{\sqrt{2\pi r}}\left(\frac{1}{4}\cos\frac{\theta}{2} + \frac{3}{4}\cos\frac{3}{2}\theta\right)
\end{aligned}$$

The stresses $\sigma_{\theta\theta}$ and $\sigma_{r\theta}$ can be further simplified by using

$$\cos 3x = 4\cos^3 x - 3\cos x$$
$$\sin 3x = 3\sin x - 4\sin^3 x$$

as follows:

$$\begin{aligned}\sigma_{\theta\theta} &= \frac{1}{\sqrt{2\pi r}}\cos\frac{\theta}{2}\left[K_I\cos^2\frac{\theta}{2} - \frac{3}{2}K_{II}\sin\theta\right] \\ \sigma_{r\theta} &= \frac{1}{\sqrt{2\pi r}}\cos\frac{\theta}{2}\left[\frac{1}{2}K_I\sin\theta + \frac{1}{2}K_{II}(3\cos\theta - 1)\right]\end{aligned} \tag{5.9}$$

It follows from these stress expressions that

$$\frac{\partial\sigma_{\theta\theta}}{\partial\theta} = -\frac{3}{2}\sigma_{r\theta}$$

which means that $\sigma_{\theta\theta}$ reaches its maximum $(\sigma_{\theta\theta})_{\max}$ at $\theta = \theta_0$ where $\sigma_{r\theta} = 0$. The crack initiation angle θ_0 (measured from the x-axis) thus satisfies the following equation:

$$\cos\frac{\theta_0}{2}\left[K_I\sin\theta_0 + K_{II}(3\cos\theta_0 - 1)\right] = 0 \tag{5.10}$$

or

$$\begin{aligned}\cos\frac{\theta_0}{2} &= 0 \\ K_I\sin\theta_0 + K_{II}(3\cos\theta_0 - 1) &= 0\end{aligned} \tag{5.11}$$

The solutions of the first equation in Eq. (5.11) are $\theta_0 = \pm\pi$, which correspond to the crack surfaces where $\sigma_{\theta\theta} = 0$. Hence, the fracture angle should be determined from the second equation in Eq. (5.11).

Now we turn to the determination of fracture load. According to the assumption of Erdogan and Sih [5-3] that fracture takes place when $(\sigma_{\theta\theta})_{\max}$ satisfies

$$(\sigma_{\theta\theta})_{\max} = \frac{K_{Ic}}{\sqrt{2\pi r}}$$

Then substituting the first expression in Eq. (5.9) (at $\theta = \theta_0$) into this condition yields the fracture criterion satisfied by K_I and K_{II}:

$$K_I\cos^2\frac{\theta_0}{2} - \frac{3}{2}K_{II}\sin\theta_0 = K_{Ic}/\cos\frac{\theta_0}{2} \tag{5.12}$$

Equations (5.11) and (5.12) are the mixed mode fracture conditions in the maximum stress criterion. It is noted that only one material property, K_{Ic}, appears in the criterion.

Consider two special cases: Mode I and Mode II, respectively. For Mode I, $K_{II} = 0$, the crack extension direction is obtained from Eq. (5.11) as

$$\theta_0 = 0$$

that is, the crack extends in its original direction. For Mode II, $K_I = 0$, and the crack growth direction is now determined as

$$\theta_0 = \arccos(1/3) \approx -70.5^0$$

5.3 STRAIN ENERGY DENSITY CRITERION (S-CRITERION)

Sih [5-4] proposed a mixed mode fracture criterion based on the strain energy density concept. For a two-dimensional cracked body, the strain energy stored in an element $dV = dxdy$ of unit thickness is

$$dU = \left[\frac{1}{2\mu}\left(\frac{\kappa+1}{8}\left(\sigma_{xx}^2+\sigma_{yy}^2\right) - \frac{3-\kappa}{4}\sigma_{xx}\sigma_{yy} + \sigma_{xy}^2\right)\right]dV$$

where $\kappa = 3-4\nu$ for plane strain and $\kappa = (3-\nu)/(1+\nu)$ for plane stress. Substituting the the crack tip stress field Eq. (5.8) for I/II mixed mode into the preceding expression, we have the strain energy density function in the form

$$\frac{dU}{dV} = W = \frac{1}{r}\left(a_{11}K_I^2 + 2a_{12}K_IK_{II} + a_{22}K_{II}^2\right) \tag{5.13}$$

where the coefficients a_{ij} $(i,j = 1,2)$ are given by

$$\begin{aligned} a_{11} &= \frac{1}{16\mu\pi}[(\kappa - \cos\theta)(1+\cos\theta)] \\ a_{12} &= \frac{1}{16\mu\pi}\sin\theta[2\cos\theta - (\kappa-1)] \\ a_{22} &= \frac{1}{16\mu\pi}[(\kappa+1)(1-\cos\theta) + (1+\cos\theta)(3\cos\theta - 1)] \end{aligned} \tag{5.14}$$

Equation (5.13) indicates that the strain energy density function has a $1/r$ singularity near the crack tip and the field intensity can be represented by the following strain energy density factor introduced by Sih [5-4]:

$$S = a_{11}K_I^2 + 2a_{12}K_IK_{II} + a_{22}K_{II}^2 \tag{5.15}$$

It is noted that the strain energy density factor S is a function of θ.

The fundamental hypotheses of the strain energy density criterion are (1) the crack will extend in the direction of minimum strain energy density (with respect to θ); and (2) crack extension occurs when the minimum strain energy density factor, $S = S_{\min}$, reaches a critical value, say S_{cr}.

It is seen from Eqs. (5.13) and (5.15) that the strain energy density W and the strain energy density factor S have the same θ-dependence. Hence, the sufficient and

necessary conditions for W to take the minimum value at $\theta = \theta_0$ are

$$\frac{\partial S}{\partial \theta} = 0 \quad \text{at } \theta = \theta_0 \tag{5.16}$$

$$\frac{\partial^2 S}{\partial \theta^2} > 0 \quad \text{at } \theta = \theta_0 \tag{5.17}$$

Equations (5.16) and (5.17) determine the crack extension angle θ_0. The fracture initiation condition is then characterized by

$$S(\theta_0) = S_{cr} \tag{5.18}$$

We now apply the strain energy density criterion to two special cases, that is, an infinite plate with a central crack subjected to remote tension σ (Mode I) and shear τ (Mode II), respectively.

Mode I

For the Mode I problem shown in Figure 5.4, we have

$$K_I = \sigma_0 \sqrt{\pi a}, \quad K_{II} = 0$$

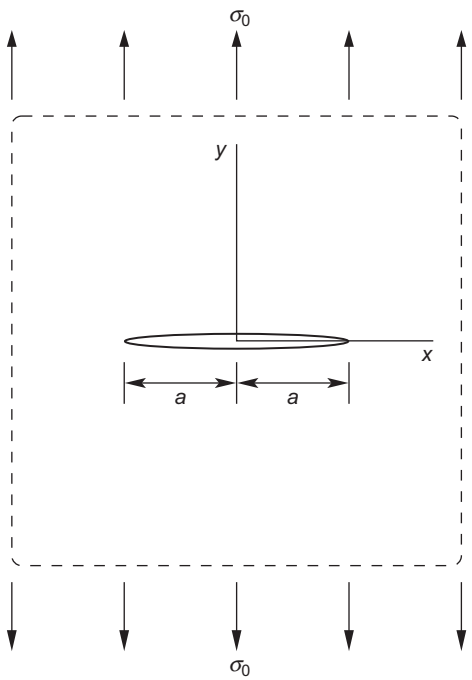

FIGURE 5.4

Crack initiation angle ($\theta_0 = 0$) in Mode I.

and

$$S = \frac{\sigma_0^2 a}{16\mu}(1+\cos\theta)(\kappa-\cos\theta)$$

The necessary condition for S to take the minimum is

$$\frac{\partial S}{\partial \theta} = 0 \;\Rightarrow\; \sin\theta\,[2\cos\theta - (\kappa-1)] = 0$$

This equation has two solutions: $\theta_0 = 0$ and $\theta_0 = \arccos[(\kappa-1)/2]$. Because

$$\frac{\partial^2 S}{\partial \theta^2} > 0 \quad \text{at } \theta_0 = 0$$

$$\frac{\partial^2 S}{\partial \theta^2} < 0 \quad \text{at } \theta_0 = \arccos\left(\frac{\kappa-1}{2}\right)$$

S thus takes the minimum at $\theta_0 = 0$, that is, the crack grows in its original direction. The minimum value of S can be obtained as

$$S_{\min} = \frac{(\kappa-1)\sigma_0^2 a}{8\mu} \quad \text{at } \theta_0 = 0^\circ$$

From this value and the second hypothesis we get the critical applied stress:

$$\sigma_{cr} = [8\mu S_{cr}/(\kappa-1)a]^{1/2}$$

The critical value S_{cr} can be related to the fracture toughness K_{Ic}. For plane strain ($\kappa = 3-4\nu$),

$$K_{Ic}^2 = \left(\sigma_{cr}\sqrt{\pi a}\right)^2 = [4\mu\pi/(1-2\nu)]\,S_{cr}$$

Hence

$$S_{cr} = \frac{1-2\nu}{4\mu\pi}K_{Ic}^2$$

Mode II

For the Mode II problem as shown in Figure 5.5, we have

$$K_I = 0, \quad K_{II} = \tau_0\sqrt{\pi a}$$

$$S = \frac{\tau_0^2 a}{16\mu}[(\kappa+1)(1-\cos\theta) + (1+\cos\theta)(3\cos\theta-1)]$$

For S to take the minimum, we have

$$\frac{\partial S}{\partial \theta} = 0 \;\Rightarrow\; \sin\theta\,[(\kappa-1) - 6\cos\theta] = 0$$

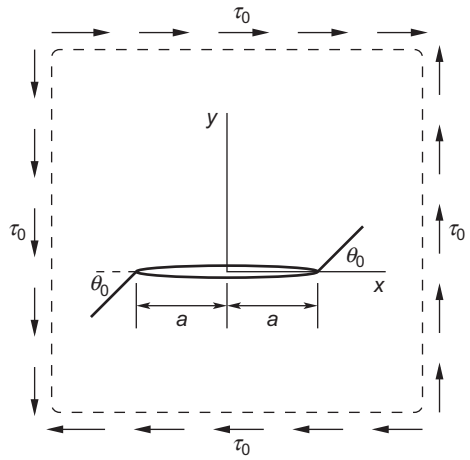

FIGURE 5.5

Crack initiation angle (θ_0) in Mode II.

Table 5.1 Crack Initiation Angle in Mode II Based on the S-Criterion

ν	0.0	0.1	0.2	0.3	0.4	0.5
θ_0	−70.5°	−75.6°	−79.3°	−83.3°	−87.2°	−90.0°

The preceding equation has two sets of solutions:

$$\theta_0 = 0$$

$$\theta_0 = \mp \arccos\left(\frac{\kappa - 1}{6}\right)$$

It can be verified that the solution $\theta_0 = 0$ gives $S_{\max}$ and the second set of solutions gives $S_{\min}$. The solution with a positive sign is discarded since in that direction $\sigma_{\theta\theta}$ is negative. The crack extension direction is thus given by

$$\theta_0 = -\arccos\left(\frac{\kappa - 1}{6}\right) \tag{5.19}$$

The corresponding S is

$$S_{\min} = \frac{(14\kappa - 1 - \kappa^2)\tau_0^2 a}{192\mu}$$

Equation (5.19) shows that the crack extension direction depends on Poisson's ratio. Table 5.1 gives some values of θ_0 for different values of Poisson's ratio under plane

strain conditions. It is noted that according to the maximum tensile stress criterion, the crack initiation angle is $\theta_0 = -70.5^\circ$, which corresponds to a material with zero Poisson's ratio in the table.

5.4 MAXIMUM ENERGY RELEASE RATE CRITERION (ME-CRITERION)

The maximum energy release rate criterion is an extension of the Griffith fracture theory in that the crack will grow in the direction along which the maximum potential energy is released. A rigorous analysis of the energy release under mixed mode conditions requires consideration of a small kink from the original main crack tip, as shown in Figure 5.6, where α is the kink angle. Denote by k_I and k_{II} the stress intensity factors at the kinked crack tip. The energy release rate at the kink tip is thus

$$G_{kink} = \frac{\kappa + 1}{8\mu}\left(k_I^2 + k_{II}^2\right) \tag{5.20}$$

Clearly, k_I and k_{II}, and hence G_{kink}, are functions of the kink angle α.

To study the crack growth direction, it is sufficient to consider a small kink, or more precisely, a kink with a length much smaller than the size of the K-dominance zone around the main crack tip. Under these considerations, k_I and k_{II} may be expressed in terms of K_I and K_{II} (stress intensity factors at the main crack tip), and the kink angle α as follows:

$$\begin{aligned} k_I &= C_{11}(\alpha)K_I + C_{12}(\alpha)K_{II} \\ k_{II} &= C_{21}(\alpha)K_I + C_{22}(\alpha)K_{II} \end{aligned} \tag{5.21}$$

where C_{ij} $(i,j = 1,2)$ are functions of α. Determination of these functions generally requires analyses of a branched crack problem as shown in Figure 5.6. Using a

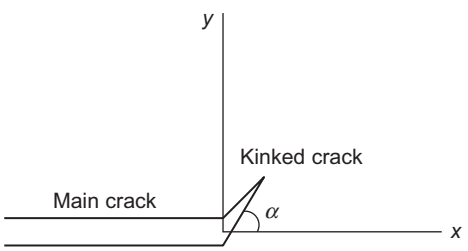

FIGURE 5.6

Crack kink in a mixed mode field.

complex stress function method, Hussain et al. [5-5] found the following expression for $C_{ij}(\alpha)$:

$$\begin{pmatrix} C_{11} & C_{12} \\ C_{21} & C_{22} \end{pmatrix} = \left(\frac{\pi-\alpha}{\pi+\alpha}\right)^{\alpha/2\pi} \left(\frac{4}{3+\cos^2\alpha}\right) \begin{pmatrix} \cos\alpha & \frac{3}{2}\sin\alpha \\ -\frac{1}{2}\sin\alpha & \cos\alpha \end{pmatrix} \tag{5.22}$$

It is noted that the positive angle α in Eq. (5.22) is measured clockwise from the x-axis in Figure 5.6.

Nuismer [5-6] used a continuity assumption to relate the stress intensity factors at the kinked crack tip and those at the main crack tip. A relationship of the type shown in Eq. (5.21) was obtained with the C_{ij} given by

$$\begin{aligned} C_{11} &= \frac{1}{2}(1+\cos\alpha)\cos\frac{\alpha}{2} \\ C_{12} &= -\frac{3}{2}\sin\alpha\cos\frac{\alpha}{2} \\ C_{21} &= \frac{1}{2}\sin\alpha\cos\frac{\alpha}{2} \\ C_{22} &= \frac{1}{2}(3\cos\alpha-1)\cos\frac{\alpha}{2} \end{aligned} \tag{5.23}$$

The continuity assumption states that when the kinked crack length goes to zero, the stress field at the kinked crack tip approaches the stress field at the tip of the main crack before propagation. Later, Cotterell and Rice [5-7] used the small kink angle assumption and obtained the same results with the following different form of the expressions for C_{ij}:

$$\begin{aligned} C_{11} &= \frac{1}{4}\left(3\cos\frac{\alpha}{2}+\cos\frac{3\alpha}{2}\right) \\ C_{12} &= -\frac{3}{4}\left(\sin\frac{\alpha}{2}+\sin\frac{3\alpha}{2}\right) \\ C_{21} &= \frac{1}{4}\left(\sin\frac{\alpha}{2}+\sin\frac{3\alpha}{2}\right) \\ C_{22} &= \frac{1}{4}\left(\cos\frac{\alpha}{2}+3\cos\frac{3\alpha}{2}\right) \end{aligned} \tag{5.24}$$

They stated that these expressions are approximately valid for α up to 40 degrees.

Substituting Eq. (5.21) into Eq. (5.20) yields

$$\begin{aligned} G_{kink} = \frac{\kappa+1}{8\mu}\Big[&\left(C_{11}^2+C_{21}^2\right)K_I^2+\left(C_{12}^2+C_{22}^2\right)K_{II}^2 \\ &+2\left(C_{11}C_{12}+C_{21}C_{22}\right)K_IK_{II}\Big] \end{aligned} \tag{5.25}$$

The crack growth direction, or fracture angle α_0, is thus determined by maximizing $G_{kink}(\alpha)$:

$$\begin{aligned} \frac{\partial G_{kink}(\alpha)}{\partial \alpha} &= 0 \quad \text{at } \alpha = \alpha_0 \\ \frac{\partial^2 G_{kink}(\alpha)}{\partial \alpha^2} &< 0 \quad \text{at } \alpha = \alpha_0 \end{aligned} \tag{5.26}$$

With the expressions of C_{ij} given in Eq. (5.23) or Eq. (5.24), it can be verified that a local Mode I condition, that is, $k_{II} = 0$, prevails near the tip of the kinked crack with the direction determined by Eq. (5.26). Thus, the crack growth condition in the maximum energy release rate criterion can be expressed as

$$G_{kink}(\alpha_0) = G_{Ic} \tag{5.27}$$

Substituting Eq. (5.25) into the previous equation, we have

$$\begin{aligned} &\left(C_{11}^2 + C_{21}^2\right) K_I^2 + \left(C_{12}^2 + C_{22}^2\right) K_{II}^2 + 2(C_{11}C_{12} \\ &+ C_{21}C_{22}) K_I K_{II} = \frac{8\mu}{\kappa + 1} G_{Ic} \end{aligned} \tag{5.28}$$

Because k_{II} vanishes at the direction of the maximum energy release rate, the criterion Eq. (5.27) is equvalent to

$$k_I(\alpha_0) = C_{11}(\alpha_0) K_I + C_{12}(\alpha_0) K_{II} = K_{Ic} \tag{5.29}$$

Equation (5.29) is also called the local symmetry criterion (Cotterell and Rice [5-7]; Goldstein and Salganik [5-8]).

It can be shown that the fracture angles determined from Eq. (5.26) using the C_{ij} given in Eq. (5.23) or Eq. (5.24) are the same as that predicted from the maximum hoop stress criterion Eq. (5.11).

5.5 EXPERIMENTAL VERIFICATIONS

A tension panel with an inclined crack as shown in Figure 5.1 is a typical specimen to verify various mixed mode fracture criteria. In experiments, the crack length is usually very small compared with other specimen sizes so that the panel can be treated as an infinite one for the purpose of stress intensity factor calculations. Using the stress intensity factor solutions in Chapter 3 and the superposition method, the K_I and K_{II} for this problem can be obtained as

$$\begin{aligned} K_I &= \sigma_0 \sqrt{\pi a} \sin^2 \beta \\ K_{II} &= \sigma_0 \sqrt{\pi a} \sin \beta \cos \beta \end{aligned} \tag{5.30}$$

where β is the angle between the crack and the load direction.

Substitution of Eq. (5.30) into the second equation in Eq. (5.11) yields the equation of crack growth angle by the maximum stress criterion:

$$\sin\beta\sin\theta_0 + \cos\beta(3\cos\theta_0 - 1) = 0 \tag{5.31}$$

For the S-criterion, the strain energy density factor is

$$S = \sigma_0^2 a(a_{11}\sin^2\beta + 2a_{12}\sin\beta\cos\beta + a_{22}\cos^2\beta)\sin^2\beta$$

Hence, the crack growth angle satisfies

$$\frac{\partial S}{\partial\theta} = 0 \Rightarrow (\kappa - 1)\sin(\theta_0 - 2\beta) - 2\sin[2(\theta_0 - \beta)] - \sin 2\theta_0 = 0 \tag{5.32}$$

Using the maximum energy release rate criterion Eqs. (5.25) and (5.26), the fracture angle $\theta_0 = \alpha_0$ is determined by

$$G_{kink}(\alpha_0) = \frac{\kappa+1}{8\mu}\left(\sigma_0^2\pi a\right)\sin^2\beta \max_{-\pi\le\alpha\le\pi}\left\{\left(C_{11}^2 + C_{21}^2\right)\sin^2\beta + \left(C_{12}^2 + C_{22}^2\right)\cos^2\beta + (C_{11}C_{12} + C_{21}C_{22})\sin^2\beta\right\} \tag{5.33}$$

Erdogan and Sih [5-3] performed a mixed mode fracture experiment using plexiglass sheets with oblique cracks under tension as shown in Figure 5.1. The specimen sizes are $9'' \times 18'' \times 3/16''$ and the crack length is $2''$. The angle β between the crack and the load direction ranges from 30° to 80°. The initial fracture angle θ_0 at the left and right ends were measured and are denoted by $(\theta_0)_L$ and $(\theta_0)_R$, respectively. $(\theta_0)_{avg}$ is the corresponding average value. The test results are listed in Table 5.2.

Table 5.2 Measured and Calculated Values of the Fracture Angle

β		30°	40°	50°	60°	70°	80°
$(\theta_0)_L$	1	−64°	−55.5°	−50°	−40°	−29°	−17°
	2	−60°	−52°	−50°	−43.5°	−30.5°	−18°
	3	−63°	−57°	−53°	−44.5°	–	−15.5°
	4	–	−57°	−52°	−43.5°	–	–
$(\theta_0)_R$	1	−65°	−58°	−50.5°	−44°	−31.5°	−18.5°
	2	–	−53°	−52°	−40°	−31°	−17.5°
	3	−60°	−55°	−51.5°	−46°	−31.5°	−17°
	4	–	−57°	−50°	−43°	–	–
$(\theta_0)_{avg}$		−62.4°	−55.6°	−51.1°	−43.1°	−30.7°	−17.3°
MS-Criterion		−60.2°	−55.7°	−50.2°	−43.2°	−33.2°	−19.3°
S-Criterion		−63.5°	−56.7°	−49.5°	−41.5°	−31.8°	−18.5°
ME-Criterion (Eq. 5.22)		−64.6°	−60°	−54.3°	−46.6°	−36°	−20.6°

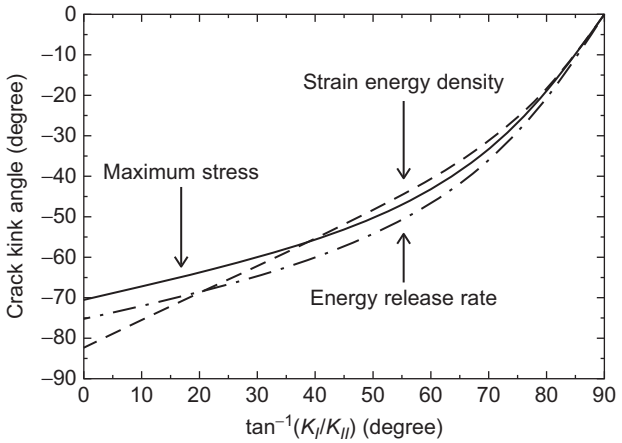

FIGURE 5.7

Fracture initiation angles predicted by the maximum tensile stress criterion, the strain energy density criterion, and the maximum energy release rate criterion (adapted from Hussain et al. [5-5]).

Also listed in the table are the theoretical predictions based on the maximum tensile stress criterion Eq. (5.31), the strain energy density criterion Eq. (5.32), and the maximum energy release rate criterion Eq. (5.33). For the maximum energy release rate criterion, only the C_{ij} given by Hussain et al. Eq. (5.22) are used since those given by Nuismer Eq. (5.23) and Cotterell and Rice Eq. (5.24) result in the same fracture angles as predicted by the maximum tensile stress criterion. It can be seen from the table that all theoretical predictions of the fracture angles are in good agreement with the experimental results.

Figure 5.7 shows the fracture angles versus the mixed mode phase angle $\tan^{-1}(K_I/K_{II})$ as predicted by the maximum tensile stress criterion, the strain energy density criterion, and the maximum energy release rate criterion. It can be observed that predictions of the strain energy density criterion deviate from those by the maximum stress and the maximum energy release rate criteria when the crack tip deformation state becomes Mode II dominated.

References

[5-1] B.C. Hoskin, D.G. Gratt, P.J. Foden, Fracture of tension panels with oblique cracks, Aeronautical Research Laboratory, Melbourne, Report SM 305, 1965.

[5-2] L.P. Pook, The effect of crack angle on fracture toughness, National Engineering Laboratory, East Kilbridge, Report NEL 449, 1970.

[5-3] F. Erdogan and G.C. Sih, On the crack extension in plates under plane loading and transverse shear, J. Basic Eng. ASME 85 (1963) 519–527.

[5-4] G.C. Sih, Strain energy density factor applied to mixed mode crack problems, Int. J. Fract. Mech. 10 (1974) 305–321.

[5-5] M.A. Hussain, S.L. Pu, J. Underwood, Strain energy release rate for a crack under combined Mode I and II, Fracture Analysis, ASTM STP 560, Am. Soc. Test. Mater. 1974, pp. 2–28.

[5-6] R.J. Nuismer, An energy release rate criterion for mixed mode fracture, Int. J. Fract. 11 (1975) 245–250.

[5-7] B. Cotterell, J.R. Rice, Slightly curved or kinked cracks, Int. J. Fract. 16 (1980) 155–169.

[5-8] R.V. Goldstein and R.L. Salganik, Brittle fracture of solids with arbitrary cracks, Int. J. Fract. 10 (1974) 507–523.

PROBLEMS

5.1 Prove that Eq. (5.10) can be obtained from $d\sigma_{\theta\theta}/d\theta = 0$.

5.2 Plot $\sigma_{\theta\theta}\sqrt{2\pi r}/K_I$ versus θ for $K_{II}/K_I = 0.5$ and 2.0, respectively. Verify that Eq. (5.11) gives the orientation at which $\sigma_{\theta\theta}$ reaches the maximum.

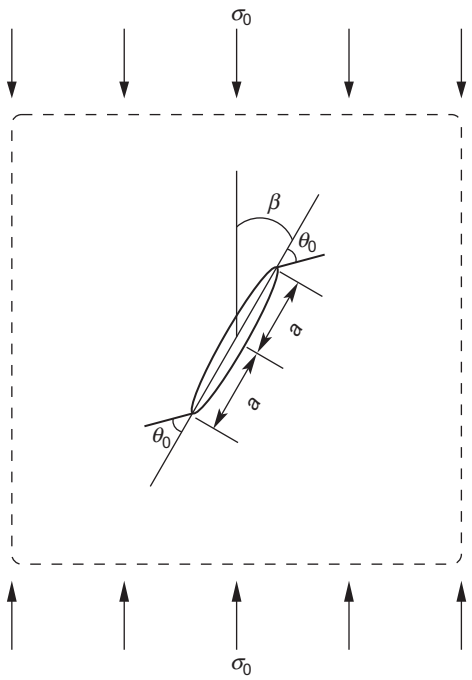

FIGURE 5.8

A compression panel with an oblique crack. The in-plane sizes of the panel are much larger than the crack length.

5.3 Plot $\sigma_{r\theta}\sqrt{2\pi r}/K_I$ versus θ for $K_{II}/K_I = 0.5$ and 2.0, respectively. Verify that $\sigma_{r\theta}$ is zero when $\sigma_{\theta\theta}$ reaches the maximum.

5.4 Show that the angle determined by $k_{II} = 0$ is along the maximum energy release rate direction.

5.5 Compare the predictions of fracture angle and failure load for a large tension panel with an oblique crack as shown in Figure 5.1. Use all methods discussed in the chapter for predictions. Assume that Poisson's ratio is 0.3 and $K_{IIc} = 1.5K_{Ic}$. Plot the results for all possible oblique angles.

5.6 Redo Problem 5.2 for a compression panel with an oblique crack as shown in Figure 5.8.